1. *Coil re-positioning*

The concurrent use of transcranial magnetic stimulation (TMS) and electroencephalogram (EEG) allows non-invasive investigation of excitability, functional connectivity and oscillatory dynamics of the cortex. A growing body of research is using this technique (TMS-EEG) to explore the current state of the neural network, particularly outside of the motor cortex. In motor cortex, relatively accurate functional targeting has been possible without the use of neuronavigation by adjusting the coil to produce maximal motor response (i.e. motor evoked potentials (MEPs)). However, targeting behaviourally silent cortical areas requires navigation techniques for precise coil positioning. It has been demonstrated TMS-evoked response in the EEG trace has a degree of sensitivity to the small changes (~1 cm) in the stimulus site (Komssi et al., 2002) and the angle of the coil (Casarotto et al., 2010). This becomes a major problem for researchers when neuronavigation system is not readily available, and often be criticized on a potentially important finding. Additionally, failure in adherence to a strict rule of coil positioning can lead to inaccurate coil position, adding more variability across similar studies.

Here, we suggest a simple method that can be adapted in an experimental setting to minimize error in coil positioning / re-positioning.

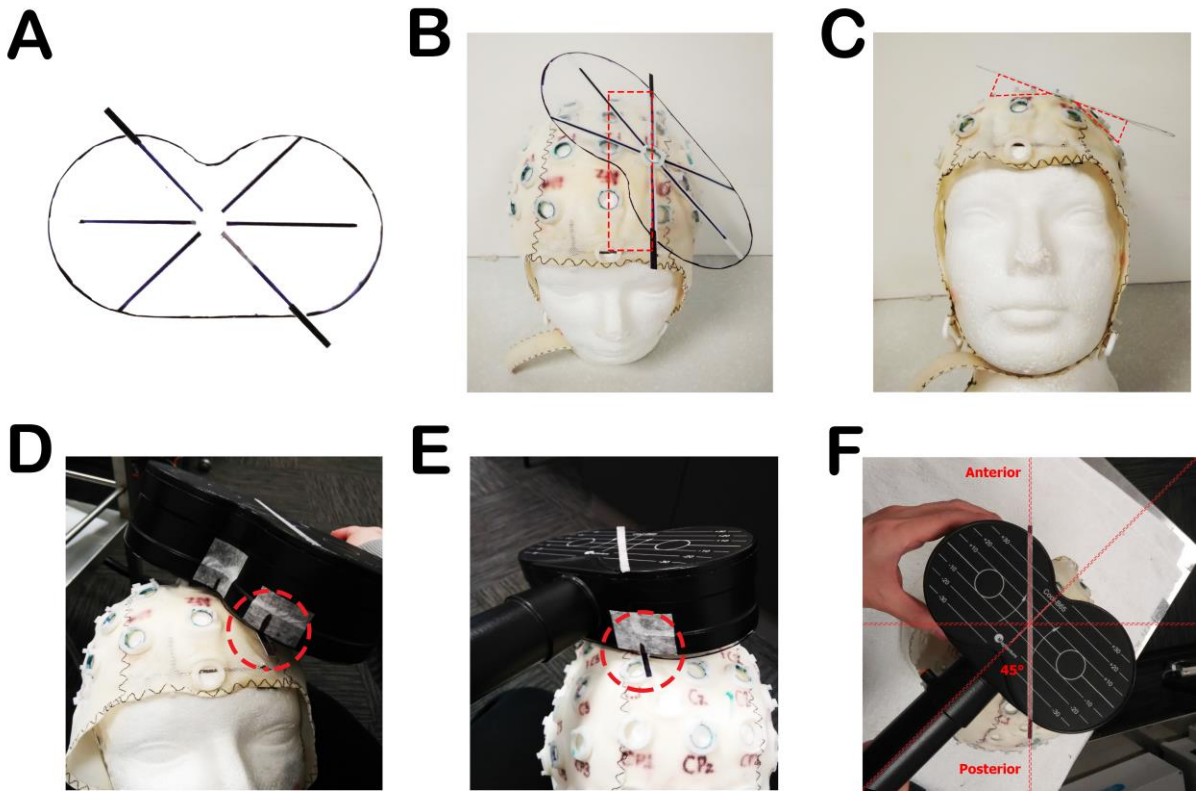

Figure S1. Use of coil template for accurate coil positioning / re-positioning based on the 10-20 system. (A) Transparent coil template customized for MagVenture B-65 fluid-cooled coil. (B) The template can be mounted on EEG cap. Red dotted rectangle indicates parallel positioning of the template to the mid-line. (C) The template provides a guide to tangential surface. TMS coil is marked to align with the template at anterior (D) and posterior (E) position. (F) Top view with coil in position.

A template of TMS coil (MagVenture B-65 fluid-cooled coil; MagVenture A/S, Denmark) was made using a transparent plastic sheet (a laminate), and lines were drawn at 45° angle (Fig S1A). The template can be secured into the rim of plastic electrode holder (i.e. F1 electrode) without increasing the distance between the cap and the coil (Fig S1B). The longer line provides a guide to 45° angle when positioned parallel to the mid-line of the EEG cap. In addition, the placement of the template is tangential to the head surface (Fig S1C). The TMS-coil is marked to align with the template at anterior (Fig S1D) and posterior (Fig S1E) site, allowing for an accurate 45° angle (Fig S1F). This method provides an accurate positioning of the coil based on the 10-20 system. More importantly, within – session reproducibility can be improved as the margin for error in re-positioning of the coil (i.e. before and after intervention) is minimized.

While this method does not provide an accurate site for individualised targets of interest (i.e. dorsolateral prefrontal cortex), placement of the coil follows strictly to the international 10-20 system. Investigative studies using an EEG cap as a guide can therefore benefit from using this method when neuronavigation is not available.

2. Comparison between MagVenture and Arduino programmed stimuli

Stimuli triggered using the Arduino microcontroller were identical to the ones programmed by MagVenture (Fig S2). The EEG were recorded during iTBS using 50 Hz / 5 Hz protocol (Huang et al., 2005).

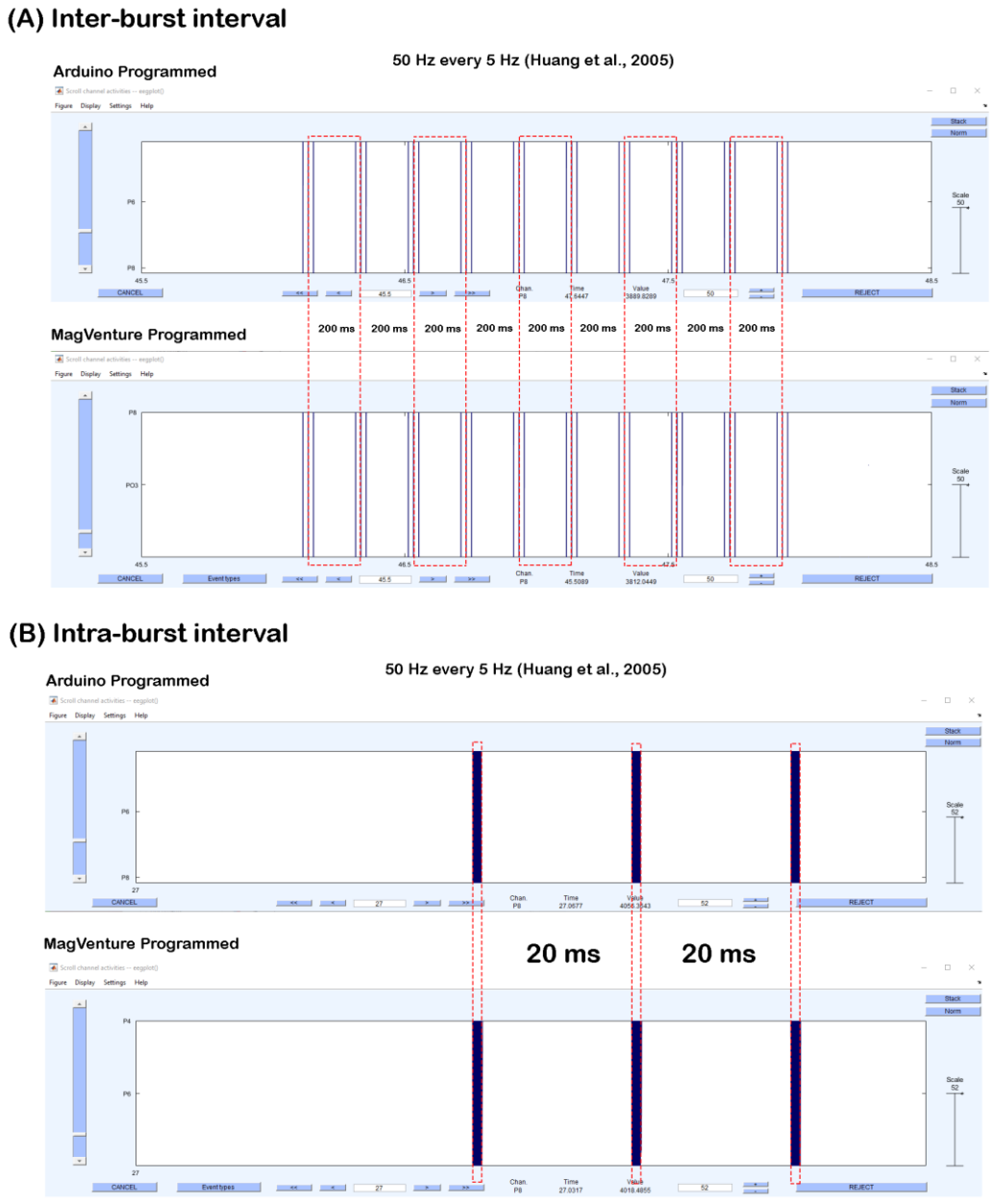

Figure S2. Comparison between MagVenture and Arduino programmed stimuli in electroencephalography (EEG) recording. (A) Inter-burst interval (5 Hz / 200 ms) and (B) Intra-burst interval (50 Hz / 20 ms). Red dotted boxes were drawn to illustrate how precisely pulses match.

3. Selection of individualised frequencies of iTBS based on theta-gamma coupling

The individualised frequency for Ind iTBS was determined by the phase-amplitude cross-frequency coupling (PAC) between frontal theta (phase) and parietal gamma (amplitude) oscillations during the 3-back task. The reasons for choosing between-channel TGC instead of within channel TGC include the observation of cross-frequency coupling between frontal theta and posterior gamma oscillations during working memory in human (Friese et al., 2013; Koster et al., 2014), increased fronto-parietal connectivity in theta and elevated parietal gamma power during working memory task following iTBS (Hoy et al., 2016), and increased frontal theta and parietal gamma power during TMS-EEG following iTBS (Chung et al., 2017). In addition, within-channel PAC is more likely to result in positive coupling due to a common driver which influences both neuronal generators instead of a direct interaction between them (Aru et al., 2015).

3-back EEG data were preprocessed off-line as described in Section 2.9. Several steps were taken to minimize common errors and to enhance the specificity of TGC using the recommendations of (Aru et al., 2015): (1) presence of a clear theta peak was verified; (2) adaptive filtering was used for the selection of bandwidths; (3) only the maintenance period of each epoch (indicated with red asterisks in Fig 2A) were included in the final calculation of TGC to avoid spurious coupling due to visual-evoked responses. As such, the beginning and end of each epoch (500 ms on each side) were discarded to prevent edge effects of filtering (for example, 'H's in Fig 2A); (4) between-channel TGC was used as cross-channel coupling is less likely to occur by a driving input to a single area.

Ten correct trials were selected by randomly ordering the epochs and using the first 10 epochs after shuffling for TGC (Fig 2A). This was to ensure that same amount of data were used for all participants while maintaining enough data length for a reliable estimation (10 cycles of the slowest oscillation (4 Hz); 10 x 0.25 = 2.5 s). Total length of data used in PAC estimation was 10 (epochs) x 4.5 (red asterisks in Fig 2A) = 45 s. The raw signals were zero-padded, concatenated and filtered (Butterworth, second-order, zero-phase) at the respective frequencies; 3 – 9 Hz for theta (Fz electrode) and 20 – 70 Hz for gamma (Pz electrode). Broader windows than traditional bandwidths were used to prevent any influence from the boundaries of filtering for the comodulogram matrix. For theta frequency, filters were applied in steps of 0.1 Hz with the bandwidth of 2 Hz. For gamma frequency, adaptive bandwidth filters were applied in steps of 1 Hz as accurate PAC estimation requires amplitude (gamma) filters with a bandwidth at least twice the centre frequency of the modulatory frequency (theta) (Dvorak and Fenton, 2014). Data were then subjected to Hilbert transform to obtain instantaneous phase and amplitude of the oscillatory signal components. Theta-filtered gamma amplitude envelope was then extracted prior to PAC estimation (Fig 2B). Phase-

amplitude coupling between theta and gamma was calculated using a general linear model (GLM) (Penny et al., 2008) and performed at every filter step to produce a comodulogram matrix. The comodulogram matrix was thresholded to display only significant values, and the *p*-values generated during the GLM calculation were collected and used to generate a significant mask. The masking threshold was adjusted for the number of multiple comparisons (61 theta bins * 51 gamma bins = 3,111; p_{thresh} = 0.05 * 3,111). Bins with a *p*-value greater than p_{thresh} were removed from the final comodulogram (white areas in Supplementary Material, Fig S3) such that only significant PAC values were considered in the final frequency estimates. The peak of the comodulogram matrix was used to infer the specific frequencies within the theta (4 – 8 Hz) and gamma (30 – 60 Hz) bands at which the highest coupling occurred. This maximum value was automatically selected, yielding individual theta and gamma frequencies for iTBS (Fig 2C shows examples from two participants, the maximum value indicated by black asterisks). These windows of frequency bands were chosen to be comparable to other stimulation conditions and for safety reasons (not exceeding 60 Hz as high-frequency bursts may pose a greater risk of seizure (Oberman et al., 2011)). Due to time constraints, PAC was performed three times using different 10 random epochs to ensure consistent TGC. Frequencies were selected using the PAC estimation closest to the mean of the three trials. Additional PAC estimations were performed post-hoc to verify the stability of the PAC and yielded stable results across trials (Supplementary Material, Fig S3). Participants' individualised frequency of stimulation are plotted in figure 2D, with an average of gamma frequency at 41.90 ± 7.7 Hz and theta frequency at 5.97 ± 1.0 Hz. This procedure was performed for every condition to be consistent across different sessions and thereby minimising any potential differences in total duration of the experiment.

4. Stability of TGC across different trials

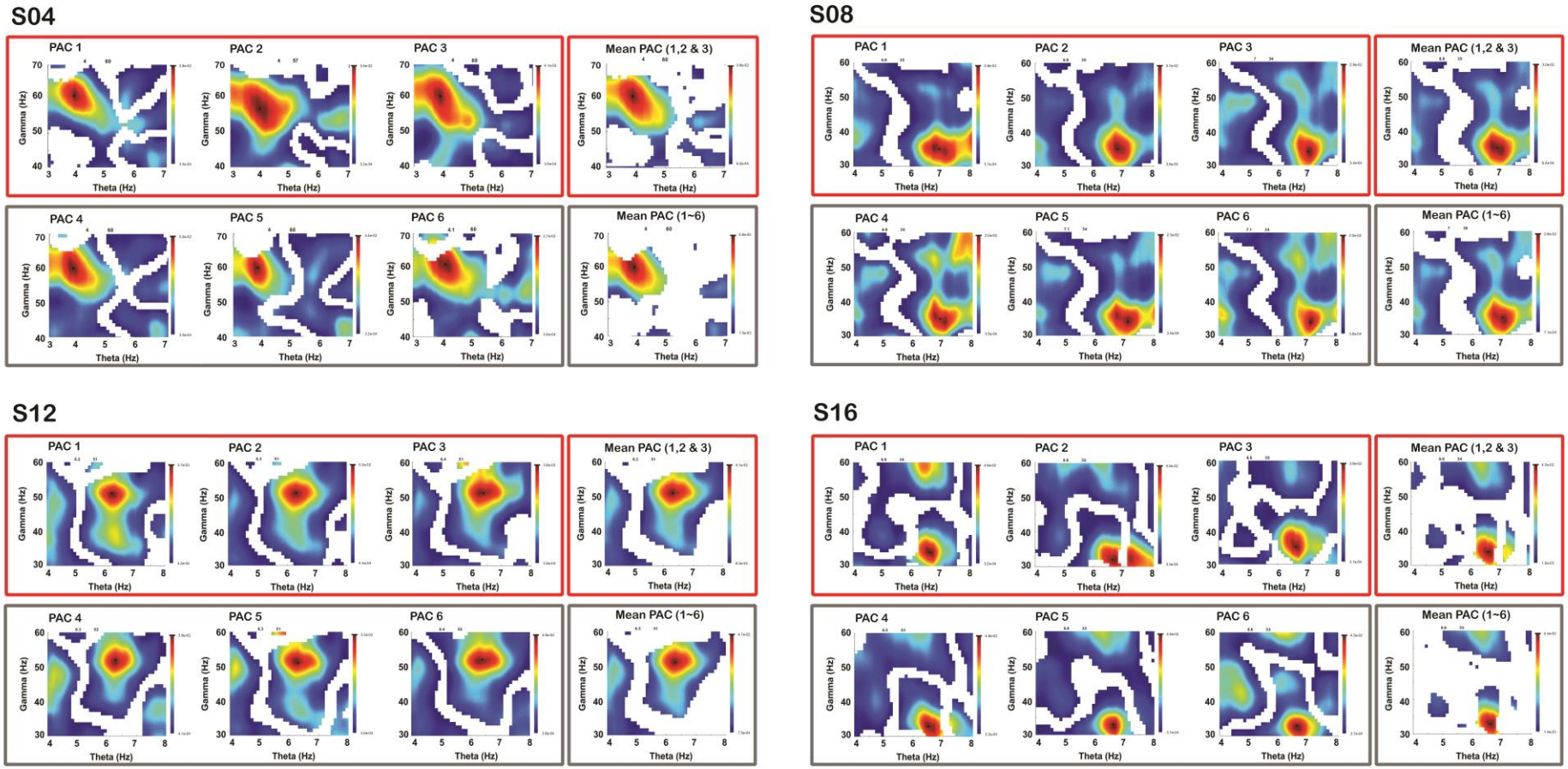

Figure S3. Stability of TGC across different trials illustrated using 4 subjects. Red boxes indicate estimation during experiment and gray boxes post-experiment for validation. Mean PAC was used as a guide for the selection of stimulation parameter and for verification. White patches indicate non-significant coupling with the threshold adjusted for the number of multiple comparisons (61 theta bins * 51 gamma bins = 3,111; p_{thresh} = 0.05 * 3,111).

5. Inter-individual variability in response to iTBS conditions

Figure S4 illustrates inter-individual variability in response to different iTBS conditions for Δ P60 and Δ N100 at T5 (black bar / left arrow) and T30 (gray bar / right arrow). There was a large variability in the number of subjects responding to 30 Hz iTBS both in the directions of iTBS-induced change [e.g. Δ P60 – T5: ↑ (n=09) ↓ (n=11); T30: ↑ (n=10) ↓ (n=10)] and over time (↑↓ & ↓↑) (Fig S4A & B). Even though 50 Hz iTBS showed a large variability in the direction of the change [e.g. Δ P60 – T5: ↑ (n=08) ↓ (n=12); T30: ↑ (n=08) ↓ (n=12)], only small number of volunteers responded differently over time (↑↓ & ↓↑) (Fig S4C & D). For Ind iTBS, both variability in the direction of the change and over time were relatively small (Fig S4E & F).

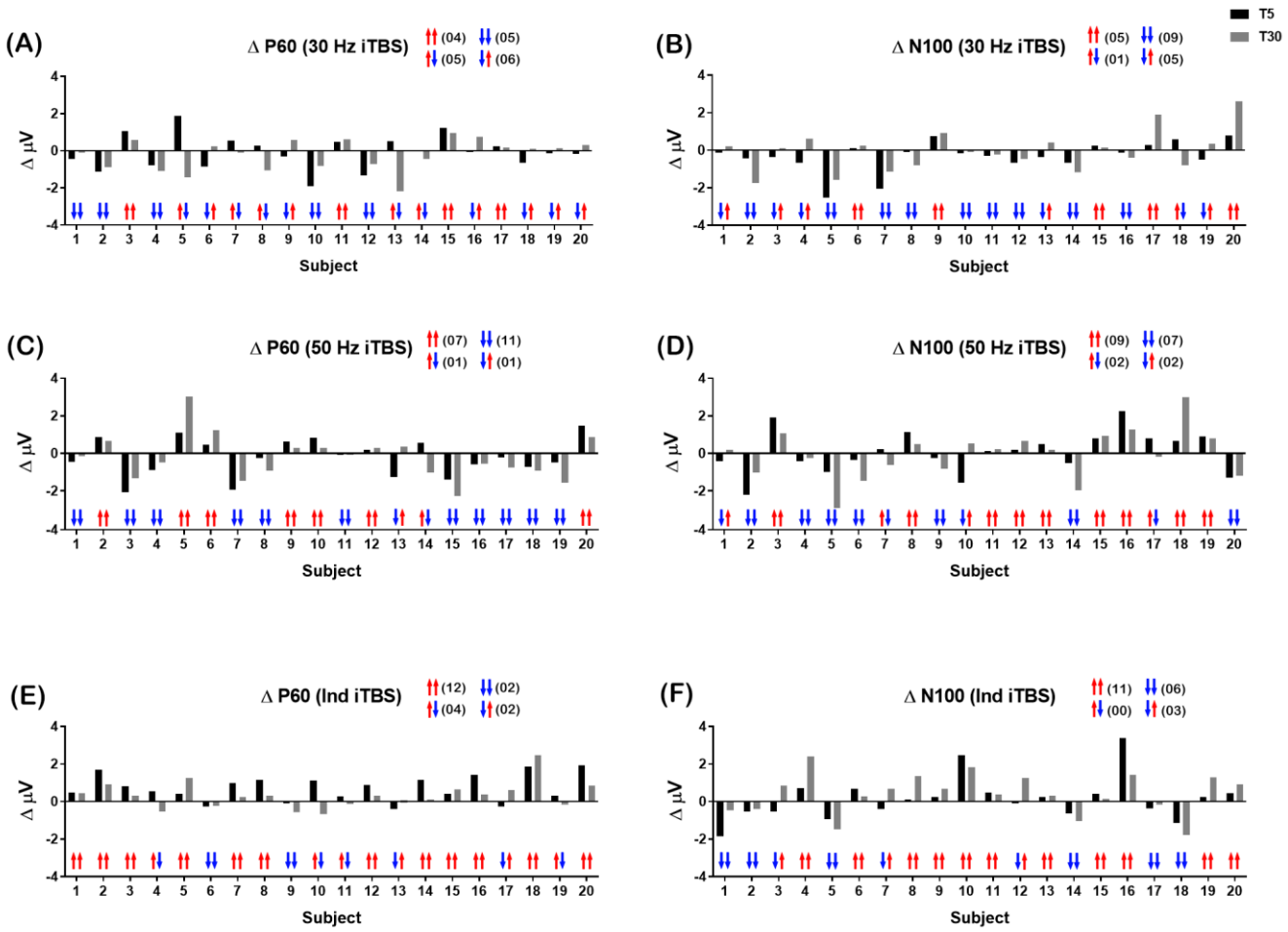

Figure S4. Inter-individual variability in response to different intermittent theta-burst stimulation (iTBS) conditions [(A-B) 30 Hz iTBS; (C-D) 50 Hz iTBS; and (E-F) Ind iTBS] in Δ P60 and Δ N100. Arrows indicate increase (↑) or decrease (↓) in the amplitude from baseline. First arrow indicates T5 and second arrow indicates T30.

6. Detailed analyses on mood scores following different stimulation conditions

Table S1. Comparison of the effect sizes and the observed power of mood rating between active conditions using change-from-baseline scores.

Δ mood	**T 60**		
One-way ANOVA	**$F_{2,38}$ = 5.495, p = 0.008, η^2 = 0.224, Power = 0.821**		
Δ mood	**Paired T-test**	**Hedges' *g* (95% CI)**	**Power**
Ind vs 30 Hz	**t = 2.966, p = 0.008***	**0.76 (0.12 1.40)**	**0.897**
Ind vs 50 Hz	**t = 2.669, p = 0.015***	**0.73 (0.09 1.38)**	**0.872**
50 Hz vs 30 Hz	t = 0.032, p = 0.975	0.01 (-0.61 0.63)	0.050

* indicates significant difference ($p < 0.05$)

7. Detailed analyses on 3-back task performance (accuracy (d') and accurate reaction time(ms)) following different stimulation conditions

Table S2. Mean (SD) *d'*, accurate reaction time (ms), the effect sizes (hedges' *g*) and the observed power of 3-back after different stimulation conditions.

		BL	T20	Hedges' *g* (95% CI) < BL vs T20 >	Power	T45	Hedges' *g* (95% CI) < BL vs T45 >	Power
***d'* (SD)**								
	30 Hz	2.39 (0.91)	2.42 (1.00)	0.04 (-0.58 0.66)	0.053	2.36 (0.98)	-0.03 (-0.64 0.59)	0.052
	50 Hz	2.43 (0.91)	**2.71 (0.83)***	**0.31 (-0.31 0.94)**	**0.261**	2.45 (0.80)	0.02 (-0.60 0.64)	0.051
	Ind	2.32 (0.73)	2.37 (0.74)	0.07 (-0.55 0.69)	0.060	**2.68 (0.89)***	**0.43 (-0.20 1.06)**	**0.447**
Two-way ANOVA (3x3)	**Condition**	$F_{2,38}$ = 0.982, p = 0.384, η^2 = 0.049, Power = 0.208						
	Time	$F_{2,38}$ = 2.729, p = 0.078, η^2 = 0.126, Power = 0.507						
	Interaction	**$F_{4,76}$ = 4.534, p = 0.002, η^2 = 0.193, Power = 0.930**						
Reaction time (SD)								
	30 Hz	601.65 (164.57)	602.06 (177.84)	0.00 (-0.62 0.62)	0.050	618.50 (168.10)	0.10 (-0.52 0.72)	0.071
	50 Hz	604.52 (175.59)	621.15 (175.39)	0.09 (-0.53 0.71)	0.067	657.90 (199.47)	0.28 (-0.34 0.30)	0.221
	Ind	620.37 (219.04)	612.28 (146.92)	-0.04 (-0.66 0.58)	0.053	645.12 (174.51)	0.12 (-0.50 0.74)	0.080
Two-way ANOVA (3x3)	**Condition**	$F_{2,38}$ = 0.783, p = 0.464, η^2 = 0.040, Power = 0.173						
	Time	**$F_{2,38}$ = 4.299, p = 0.021, η^2 = 0.185, Power = 0.714**						
	Interaction	$F_{4,76}$ = 0.493, p = 0.741, η^2 = 0.025, Power = 0.161						

* indicates significant difference from other time points (p < 0.05)

Table S3. Comparison of the effect sizes and the observed power of accuracy (*d'*) and accurate reaction time (ms) in the 3-back task between active conditions using change-from-baseline scores.

Δ *d'*	**T 20**			**T45**		
One-way ANOVA	$F_{2,38}$ = 2.727, p = 0.078, η^2 = 0.126, Power = 0.507			**$F_{2,38}$ = 3.463, p = 0.042*, η^2 = 0.154, Power = 0.614**		
	< BL vs T20 >			**< BL vs T45 >**		
Δ *d'*	**Paired T-test**	**Hedges' *g* (95% CI)**	**Power**	**Paired T-test**	**Hedges' *g* (95% CI)**	**Power**
Ind vs 30 Hz	t = 0.152, p = 0.881	0.05 (-0.57 0.67)	0.055	**t = 2.102, p = 0.049***	**0.64 (0.01 1.28)**	**0.775**
Ind vs 50 Hz	t = -2.063, p = 0.053	-0.62 (-1.25 0.02)	0.749	**t = 2.156, p = 0.044***	**0.75 (0.08 1.36)**	**0.889**
50 Hz vs 30 Hz	t = 1.997, p = 0.060	0.54 (-0.09 1.17)	0.630	t = 0.309, p = 0.760	0.08 (-0.54 0.70)	0.656
Δ Reaction time	**T20**			**T45**		
One-way ANOVA	$F_{2,38}$ = 0.371, p = 0.693, η^2 = 0.019, Power = 0.105			$F_{2,38}$ = 0.793, p = 0.460, η^2 = 0.040, Power = 0.175		
	< BL vs T20 >			**< BL vs T45 >**		
Δ ms	**Independent T-test**	**Hedges' *g* (95% CI)**	**Power**	**Independent T-test**	**Hedges' *g* (95% CI)**	**Power**
Ind vs 30 Hz	t = -0.250, p = 0.806	-0.08 (-0.70 0.54)	0.063	t = -0.910, p = 0.374	0.08 (-0.54 0.71)	0.063
Ind vs 50 Hz	t = -0.887, p = 0.386	-0.24 (-0.86 0.38)	0.175	t = 0.298, p = 0.769	-0.29 (-0.92 0.33)	0.234
50 Hz vs 30 Hz	t = 0.653, p = 0.522	0.20 (-0.42 0.83)	0.136	t = 1.100, p = 0.285	0.39 (-0.24 1.01)	0.381

* indicates significant difference (p < 0.05)

8. *Inter-individual variability in working memory performance (d' and reaction time) in response to iTBS conditions*

Figure S5 illustrates inter-individual variability in response to different iTBS conditions for Δ accuracy (*d'*) and Δ reaction time (ms) at T20 (black bar) and T45 (gray bar). There was a large variability in the number of subjects responding to 30 Hz iTBS in the directions of iTBS-induced change in Δ *d'* (T20: ↑ (n=10) ↓ (n=10); T45: ↑ (n=8) ↓ (n=10)] (Fig S5A). 50 Hz iTBS and Ind iTBS showed reduced variability in Δ *d'* at T20 (↑ (n=13) ↓ (n=7)) and T45 (↑ (n=14) ↓ (n=6)), respectively (Fig S5C & 5E). In general, reduced reaction time was not evident across different iTBS conditions (Fig 5B, 5D & 5F).

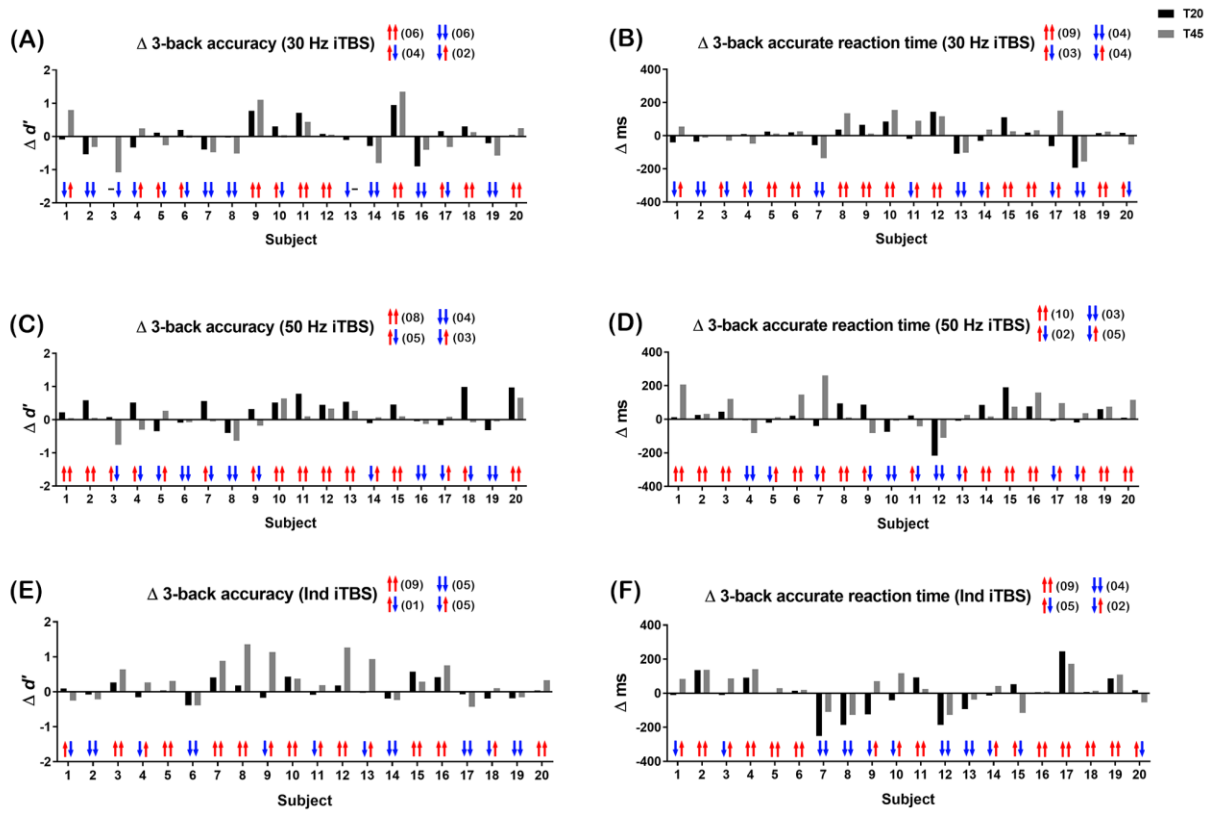

Figure S5. Inter-individual variability in response to different intermittent theta-burst stimulation (iTBS) conditions [(A-B) 30 Hz iTBS; (C-D) 50 Hz iTBS; and (E-F) Ind iTBS] in Δ *d'* and Δ ms. Arrows indicate increase (↑) or decrease (↓) in the accuracy / reaction time relative to baseline. First arrow indicates T20 and second arrow indicates T45.

9. Control analysis

To validate the statistical method used for the comparison of TEPs in this study (nonparametric cluster-based permutation statistics), 3 (iTBS condition) x 3 (time) repeated measures ANOVA was performed using the data extracted from 6 frontal electrodes (F1, Fz, F2, FC1, FCz and FC2) as described in section 2.12.

For P60 amplitude, a significant main effect of condition ($F_{2,38}$ = 7.433, p = 0.002) and a significant interaction ($F_{4,76}$ = 4.680, p = 0.002) were observed, however, no significant main effect of time was found ($F_{2,38}$ = 1.545, p = 0.227). In order to investigate the interaction effect, a series of one-way ANOVAs was performed. Within condition comparisons yielded a significant main effect of time in Ind iTBS condition ($F_{2,38}$ = 7.419, p = 0.002). Post-hoc pairwise comparisons (Bonferroni corrected) revealed that P60 amplitude was significantly higher at T5 (p = 0.003) and T30 (p = 0.027) compared to BL. No significant main effect of time was found in 30 Hz ($F_{2,38}$ = 0.775, p = 0.468) and 50 Hz iTBS conditions ($F_{2,38}$ = 2.020, p = 0.147). Across conditions, a significant main effect was found at T5 ($F_{2,38}$ = 8.762, p = 0.001) and at T30 ($F_{2,38}$ = 5.526, p = 0.008). Post-hoc pairwise comparisons revealed that P60 amplitude was significantly higher following Ind iTBS compared to both 30 Hz (T5 – p = 0.024; T30 – p = 0.046) and 50 Hz iTBS (T5 – p = 0.001; T30 – p = 0.031). No significant main effect was found at BL ($F_{2,38}$ = 0.055, p = 0.946).

For N100 amplitude, no significant main effects of condition ($F_{2,38}$ = 1.004, p = 0.376) or time ($F_{2,38}$ = 0.876, p = 0.425) were found. However, a significant interaction was observed ($F_{4,76}$ = 2.662, p = 0.039). Within condition comparisons using one-way ANOVAs yielded a significant main effect of time in Ind iTBS condition ($F_{2,38}$ = 8.621, p = 0.001). Post-hoc pairwise comparisons (Bonferroni corrected) revealed that N100 amplitude was smaller at T5 (p = 0.064) and T30 (p = 0.008) compared to BL. No significant main effect of time was found in 30 Hz ($F_{2,38}$ = 0.032, p = 0.969) and 50 Hz iTBS conditions ($F_{2,38}$ = 1.516, p = 0.232). Across conditions, no significant main effect was found at T5 ($F_{2,38}$ = 1.142, p = 0.330) and at T30 (a trend; $F_{2,38}$ = 2.690, p = 0.081). No significant main effect was found at BL ($F_{2,38}$ = 0.552, p = 0.580).

For P200 amplitude, no significant main effects or interaction were observed [Condition – ($F_{2,38}$ = 0.600, p = 0.554); Time – ($F_{2,38}$ = 0.315, p = 0.732); Interaction – ($F_{4,76}$ = 1.430, p = 0.232)].

10. Secondary analyses of sham condition

Twelve age and gender-ratio matched volunteers (4 female, 26.0 ± 6.2 years of age, 16.0 ± 2.26 years of formal education) were included in the study as a control condition for a secondary analysis where application of active stimulation was absent. The analyses were performed on data which were collected in a previous study (https://doi.org/10.1016/j.brs.2018.01.002). The protocols were very similar to the current study, with the same time frame for single-pulse TMS measurement (T5 & T30) followed by working memory performance. Sham iTBS (50 Hz at 5 Hz) was applied at 90° tilt with bottom of the TMS coil facing away from the scalp.

For mood and working memory performance, simple independent t-tests were used to compare active conditions to sham using change-from-baseline values (Δ) rather than absolute values because of; a) differences in the number of samples (20 vs 12) and population (repeated vs independent) and b) differences in baseline values as a result of different population.

TMS-EEG

No significant differences in TEPs were found following sham stimulation (Fig S5A). For comparison across conditions (using independent t-tests), significant differences were found between Ind iTBS and Sham condition [N45 (T5: $p = 0.005$), P60 (T5: $p = 0.001$; T30: $p = 0.019$), N100 (T30: $p = 0.016$), P200 (T5: $p = 0.021$)] (Fig S5B). No significant differences were found between sham condition and 30 / 50 Hz iTBS (all $p > 0.025$).

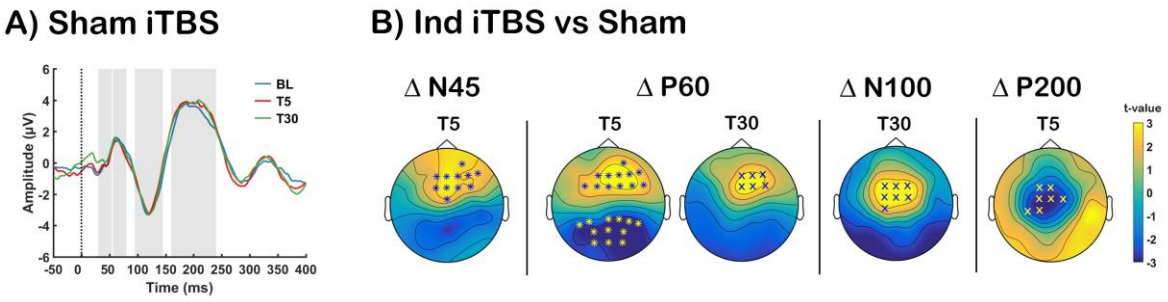

Figure S5. Assessment of transcranial magnetic stimulation (TMS)-evoked potentials (TEPs) following sham stimulation. Grand average TEP waveforms at baseline (BL: blue), 5-min post (T5: red) and 30-min post (T30: green) using 3 fronto-central electrodes (FC1, FCz and FC2). (B) Topoplots represent t-values for comparison between Ind iTBS and sham stimulation (cluster-based statistics, $*p < 0.01$, $^{X}p < 0.025$).

Mood rating

No overall change in mood was visible following sham stimulation (Fig S6). Independent samples t-tests revealed significant differences between Ind iTBS and sham stimulation (p = 0.006). No significant differences were found between sham stimulation and 30 Hz (p = 0.506) or 50 Hz iTBS (p = 0.509).

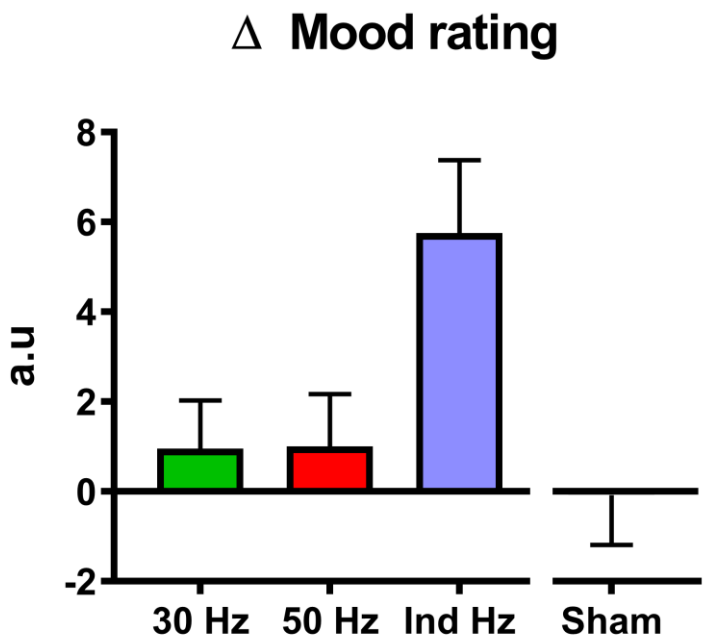

Figure S6. Visualisation for the effect of sham stimulation on the change in mood rating. Error bars indicate standard error of means (SEM).

Table S4. Mean (SD) mood rating, the effect sizes (hedges' *g*) and the observed power following sham stimulation and its comparison to active stimulation conditions using change-from-baseline scores.

Mood rating (SD)	**BL**	**T60**	**Hedges' *g* (95% CI)**	***t(p)***
Sham	68.08 (11.81)	68.00 (10.95)	0.01 (-0.79 0.81)	0.075 (0.941)
Δ *d'*	**Independent T-test**	**Hedges' *g* (95% CI)**	**Power**	
30 Hz vs Sham	t = 0.623, p = 0.538	0.22 (-0.50 0.94)	0.090	
50 Hz vs Sham	t = 0.631, p = 0.533	0.22 (-0.49 0.94)	0.090	
Ind vs Sham	**t = 2.967, p = 0.006***	**0.91 (0.16 1.66)**	**0.674**	

* indicates significant difference (p < 0.05)

3-back task

Figure S7 depcits the change-from-baseline scores of working memory performance following different iTBS conditions, separated by sham condition for visualisation purposes. No significant changes in working memory performance (*d'* and accurate reaction time) were found following sham stimulation over time (all $p > 0.05$). Independent samples t-tests revealed significant differences in *d'* between Ind iTBS and sham stimulation at T30 ($p = 0.005$). No other significant differences were seen between active conditions and sham stimulation in either *d*' or accurate reaction time (all $p > 0.05$).

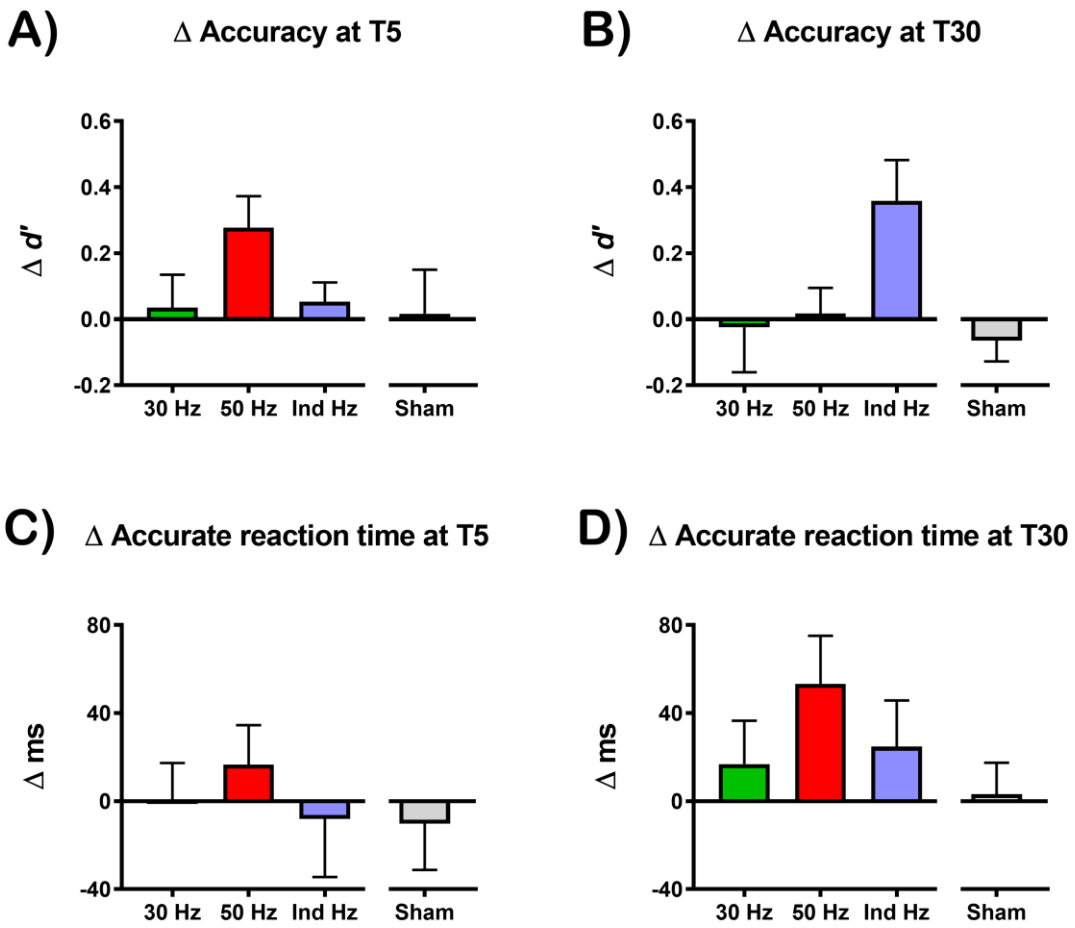

Figure S7. Change in working memory performance across different stimulation conditions. Error bars indicate standard error of means (SEM).

Table S5. Mean (SD) *d'*, accurate reaction time (ms), the effect sizes (hedges' *g*) and the observed power of the 3-back task following sham stimulation and its comparison to active stimulation conditions using change-from-baseline scores.

***d'* (SD)**	**BL**	**T20**		**T45**	$F_{2,22}$ ***(p)***	η^2
Sham	2.72 (1.01)	2.74 (1.14)		2.65 (0.97)	0.305 (0.740)	0.027
	< BL vs T20 >			**< BL vs T45 >**		
Δ *d'*	**Independent T-test**	**Hedges' *g* (95% CI)**	**Power**	**Independent T-test**	**Hedges' *g* (95% CI)**	**Power**
30 Hz vs Sham	*t* = 0.115, *p* = 0.909	0.04 (-0.67 0.76)	0.051	*t* = 0.267, *p* = 0.791	0.08 (-0.64 0.79)	0.055
50 Hz vs Sham	*t* = 1.616, *p* = 0.117	0.58 (-0.15 1.30)	0.337	*t* = 0.735, *p* = 0.468	0.26 (-0.46 0.98)	0.106
Ind vs Sham	*t* = 0.287, *p* = 0.776	0.10 (-0.61 0.82)	0.058	***t* = 3.025, *p* = 0.005***	**0.89 (0.14 1.64)**	**0.656**
Reaction time (SD)	**BL**	**T20**		**T45**	$F_{2,22}$ ***(p)***	η^2
Sham	476.40 (94.92)	466.28 (126.14)		479.52 (105.81)	0.358 (0.703)	0.032
	< BL vs T20 >			**< BL vs T45 >**		
Δ ms	**Independent T-test**	**Hedges' *g* (95% CI)**	**Power**	**Independent T-test**	**Hedges' *g* (95% CI)**	**Power**
30 Hz vs Sham	*t* = 0.385, *p* = 0.703	0.14 (-0.58 0.85)	0.066	*t* = 0.492, *p* = 0.626	0.18 (-0.54 0.89)	0.076
50 Hz vs Sham	*t* = 0.942, *p* = 0.354	0.34 (-0.38 1.06)	0.147	*t* = 1.930, *p* = 0.063	0.59 (-0.14 1.32)	0.346
Ind vs Sham	*t* = 0.053, *p* = 0.958	0.02 (-0.70 0.73)	0.050	*t* = 0.851, *p* = 0.401	0.26 (-0.46 0.98)	0.106

* indicates significant difference ($p < 0.05$)

11. Post-hoc sensitivity analyses on 3-back task using Bayesian approach

Additional post-hoc Bayesian tests were conducted using JASP software (Wagenmakers et al., 2018). Bayes Factor (BF_{10} – support in favour of H_1; BF_{01} – support in favour of H_0) denotes how likely the comparison is true. For example, the Bayes Factor was 5.282 in favour of H_1 over the two-sided H_0 for Ind iTBS (BL vs T45) (Across time; Table S6). This indicates that the observed data are 5.282 times more likely under H_1 than under H_0. Overall, Bayesian statistics showed similar outcome to the standard parametric tests.

Table S6. Comparisons of accuracy (*d'*) within and between conditions using Bayesian method.

Across time					
	< BL vs T20 >			**< BL vs T45 >**	
d'	**BF_{10}**	**BF_{01}**		**BF_{10}**	**BF_{01}**
30 Hz iTBS	0.246	4.060		0.236	4.243
50 Hz iTBS	**5.433***	0.184	(T20 > BL)	0.238	4.204
Ind iTBS	0.337	2.965		**5.282***	0.189 (T45 > BL)
Across conditions					
	< T20 >			< **T45 >**	
Δ *d'*	**BF_{10}**	**BF_{01}**		**BF_{10}**	**BF_{01}**
Ind vs 30 Hz	0.235	4.259		**1.410***	0.709 (Ind > 30 Hz)
Ind vs 50 Hz	1.327	0.753		**1.533***	0.625 (Ind > 50 Hz)
50 Hz vs 30 Hz	1.200	0.833		0.243	4.122
VS sham					
	< T20 >			< **T45 >**	
Δ *d'*	**BF_{10}**	**BF_{01}**		**BF_{10}**	**BF_{01}**
30 Hz vs Sham	0.301	3.322		0.298	3.355
50 Hz vs Sham	1.115	0.897		0.289	3.462
Ind vs Sham	0.300	3.333		**5.071***	0.197 (Ind > sham)

* indicates significant differences based on non-Bayesian statistics ($p < 0.05$)

References

Aru, J., Aru, J., Priesemann, V., Wibral, M., Lana, L., Pipa, G., Singer, W., Vicente, R., 2015. Untangling cross-frequency coupling in neuroscience. Curr Opin Neurobiol 31, 51-61.
Casarotto, S., Romero Lauro, L.J., Bellina, V., Casali, A.G., Rosanova, M., Pigorini, A., Defendi, S., Mariotti, M., Massimini, M., 2010. EEG responses to TMS are sensitive to changes in the perturbation parameters and repeatable over time. PLoS One 5, e10281.
Chung, S.W., Rogasch, N.C., Hoy, K.E., Fitzgerald, P.B., 2017. More is not always better: impact of different intensities of intermittent theta burst stimulation in prefrontal cortex using TMS-EEG. Poster session presented at the 2nd International Brain Stimulation Conference, Barcelona, Spain, p. 0231.
Dvorak, D., Fenton, A.A., 2014. Toward a proper estimation of phase-amplitude coupling in neural oscillations. J Neurosci Methods 225, 42-56.
Friese, U., Koster, M., Hassler, U., Martens, U., Trujillo-Barreto, N., Gruber, T., 2013. Successful memory encoding is associated with increased cross-frequency coupling between frontal theta and posterior gamma oscillations in human scalp-recorded EEG. Neuroimage 66, 642-647.
Hoy, K.E., Bailey, N., Michael, M., Fitzgibbon, B., Rogasch, N.C., Saeki, T., Fitzgerald, P.B., 2016. Enhancement of Working Memory and Task-Related Oscillatory Activity Following Intermittent Theta Burst Stimulation in Healthy Controls. Cereb Cortex 26, 4563-4573.
Huang, Y.Z., Edwards, M.J., Rounis, E., Bhatia, K.P., Rothwell, J.C., 2005. Theta burst stimulation of the human motor cortex. Neuron 45, 201-206.
Komssi, S., Aronen, H.J., Huttunen, J., Kesaniemi, M., Soinne, L., Nikouline, V.V., Ollikainen, M., Roine, R.O., Karhu, J., Savolainen, S., Ilmoniemi, R.J., 2002. Ipsi- and contralateral EEG reactions to transcranial magnetic stimulation. Clin Neurophysiol 113, 175-184.
Koster, M., Friese, U., Schone, B., Trujillo-Barreto, N., Gruber, T., 2014. Theta-gamma coupling during episodic retrieval in the human EEG. Brain Res 1577, 57-68.
Oberman, L., Edwards, D., Eldaief, M., Pascual-Leone, A., 2011. Safety of theta burst transcranial magnetic stimulation: a systematic review of the literature. J Clin Neurophysiol 28, 67-74.
Penny, W.D., Duzel, E., Miller, K.J., Ojemann, J.G., 2008. Testing for nested oscillation. J Neurosci Methods 174, 50-61.
Wagenmakers, E.J., Love, J., Marsman, M., Jamil, T., Ly, A., Verhagen, J., Selker, R., Gronau, Q.F., Dropmann, D., Boutin, B., Meerhoff, F., Knight, P., Raj, A., van Kesteren, E.J., van Doorn, J., Smira, M., Epskamp, S., Etz, A., Matzke, D., de Jong, T., van den Bergh, D., Sarafoglou, A., Steingroever, H., Derks, K., Rouder, J.N., Morey, R.D., 2018. Bayesian inference for psychology. Part II: Example applications with JASP. Psychon Bull Rev 25, 58-76.